Geomechanics and Engineering, *Vol. 13*, *No. 2* (*2017*) *301-318*
DOI: https://doi.org/10.12989/gae.2017.13.2.301

Three-dimensional limit analysis of seismic stability of tunnel faces with quasi-static method

B. Zhang [*1], X. Wang [1], J.S. Zhang [1] and F. Meng [2a]

[1] *School of Civil Engineering*, *Central South University*, *Hunan 410075*, *China*
[2] *Centre for Innovative Structures and Materials*, *School of Civil Engineering*, *MIT University*, *Melbourne 3001*, *Australia*

(*Received October 18*, *2016*, *Revised March 01*, *2017*, *Accepted March 11*, *2017*)

Abstract. Based on the existing research results, a three-dimensional failure mechanism of tunnel face was constructed. The dynamic seismic effect was taken into account on the basis of quasi-static method, and the nonlinear Mohr-Coulomb failure criterion was introduced into the limit analysis by using the tangent technique. The collapse pressure along with the failure scope of tunnel face was obtained through nonlinear limit analysis. Results show that nonlinear coefficient and initial cohesion have a significant impact on the collapse pressure and failure zone. However, horizontal seismic coefficient and vertical seismic proportional coefficient merely affect the collapse pressure and the location of failure surface. And their influences on the volume and height of failure mechanism are not obvious. By virtue of reliability theory, the influences of horizontal and vertical seismic forces on supporting pressure were discussed. Meanwhile, safety factors and supporting pressures with respect to 3 different safety levels are also obtained, which may provide references to seismic design of tunnels.

Keywords: tunnel face; three-dimensional collapse failure mechanism; quasi-static method; limit analysis with nonlinear failure criterion; failure probability

1. Introduction

The earthquake is a very common but unpredictable nature disaster. It not only causes damage to ground buildings but also affects the stability of underground structures. However, from a traditional point of view, the tunnel was considered to possess a better seismic performance than ground buildings. Thus, little attention has been paid to the seismic design of tunnels. In fact, the earthquake is highly destructive to tunnels (Pitilakis *et al*. 2014). During the 1995 Kobe earthquake, 30 tunnels were damaged and 10 of them were in need of repair. The Chi-Chi earthquake in 1999 broke 49 tunnels, and 25% of them were heavily damaged. During the 2008 Wenchuan earthquake, most of the tunnels in the affected area were destroyed, and the percentage of heavily damaged tunnels was up to 73% (Shen *et al*. 2014). Hence, the seismic design of tunnels cannot be ignored, and corresponding studies about the influences of earthquakes on the stability of tunnels are of great scientific values and engineering significance (Alielahi and Adampira 2016a, b).

*Corresponding author, Ph.D., E-mail: zb144801019@csu.edu.cn
[a] Ph.D. Student, E-mail: mengfei90@163.com

http://www.techno-press.org/?journal=gae&subpage=7 ISSN: 2005-307X (Print), 2092-6219 (Online)

The research methods of earthquake mainly include seismological observation, seismic experiments and theoretical analysis method (Liu *et al*. 2015). The former two methods have the disadvantages of high cost, time-consuming and restriction of geological condition. With the development of computer technology, the theoretical analysis method has been widely applied in engineering. Currently, the quasi-static method and time history analysis method are commonly utilized in the theoretical analysis of earthquake (Saada *et al*. 2013). The time history method has many merits, but the numerical modeling and analysis are complicated, which is not convenient for the engineers to master and use. On the contrary, due to the advantages of clear mechanical conception and simple calculation procedure, the quasi-static method is widely accepted (Sahoo and Kumar 2014).

In order to investigate the stability of tunnel face, its failure mechanism should be constructed. Leca and Dormieux (1990) firstly proposed a three-dimensional failure mechanism of tunnel face, which was validated by making a comparison between the theoretical results and model test data. Then it was applied to analyze the stability of tunnel face. Although this three-dimensional failure mechanism was widely accepted, it is composed of a few blocks and the accuracy of the computed result remains to be improved. Soubra (2000) introduced the logarithm spiral curve into the failure mechanism and constructed a three-dimensional multi-block failure mechanism. The obtained results are much closer to the centrifuge experiment data, which shows the logarithm spiral curve is better at presenting the failure features of tunnel face. Subsequently, based on the three-dimensional multi-block failure mechanism, Soubra (Soubra 2002, Soubra *et al*. 2008) conducted some further researches on the stability of tunnel face. Due to the advantages of logarithm spiral curve, Subrin and Wong (2002) constructed a three-dimensional log-spiral failure mechanism. The mechanism is composed of a rotational block, and its variation is determined by the center of rotation. The obtained result is consistent with the numerical simulation and is more optimal than previous result, which verifies the validity of the failure mechanism. The three-dimensional log-spiral failure mechanism is then widely adopted in the stability analysis of tunnel face, and it is usually called horn failure mechanism. However, this failure mechanism relies on too many assumptions, especially that the interface between the horn and tunnel face is assumed to be a circle, while in fact it is not a circle. Thus, the accuracy of the result is affected, and the failure mechanism needs some improvements. Mollon *et al*. (2011, 2013) have done a lot of researches on the stability of tunnel face. Firstly, based on the existing three-dimensional failure mechanisms, two multi-block failure mechanisms were proposed, namely the collapse mechanism and blow-out mechanism. Further, for the purpose of exhibiting the failure characteristic of tunnel face in a more flexible and precise way, a failure mechanism was constructed utilizing the special discretization technique. Its major advantage is the elimination of the assumptions of Subrin and Wong (2002) and the accuracy of calculation is enhanced. This mechanism was initially two-dimension and then extended to three-dimension. The shape of the mechanism is similar to a horn, but the slip surface is neither logarithm spiral curve nor any other kind of standard curve. It is determined point by point. Since the construction of the failure mechanism is rather complex, it is not convenient to promote and apply in practical engineering.

In this paper, a three-dimensional failure mechanism of tunnel face in soil masses is presented based on Michalowski (Michalowski 2010, Michalowski and Nadukuru 2013). The seismic force is introduced into the mechanical calculation by virtue of the quasi-static method. Afterward, combining the limit analysis with the reliability theory, the stability of tunnel face is investigated. The collapse pressure and failure scope under earthquake are solved, and the safety factors along with supporting pressures with respect to different safety levels are obtained.

2. Methods of analysis

2.1 The quasi-static method

The substance of the quasi-static method is equalizing the influence of dynamic force to the action of static force. As regards seismic force, its dynamic effect in the horizontal direction and vertical direction are equivalent to static forces acting on the material point, which can be represented by the horizontal seismic coefficient k_h and the vertical seismic coefficient k_v, respectively. Moreover, there is a relationship between the horizontal seismic coefficient and the vertical seismic coefficient (Saada *et al*. 2013, Sahoo and Kumar 2014)

$$k_{\mathrm{v}} = \zeta k_{\mathrm{h}} \tag{1}$$

where ζ is the vertical seismic proportional coefficient. The magnitude of ζ is generally 0.5. A positive value illustrates a downward direction, while negative denotes an upward direction. Researches have shown that a k_h in the range from 0 to 0.3 agrees well with the practical engineering. Considering the high vertical peak acceleration under strong earthquake, the value of ζ is taken as -1.0~1.0 in this paper. In order to investigate the influence of earthquake on the stability of tunnel face, the horizontal and vertical seismic forces are simplified as k_h and k_v times of the soil weight.

2.2 The tangential technique

Soil masses are frictional materials and mainly occur shear failure. The linear Mohr-Coulomb failure criterion is normally adopted to represent their shear strength. However, plenty of experiments have indicated that, as regards soil masses, the relationship between shear strength and stress state is nonlinear in fact. Thus, the nonlinear Mohr-Coulomb failure criterion is employed by many scholars (Zhang *et al*. 2014, Yang and Yan 2015), which can be expressed as

$$\tau = c_0 \left(1 + \sigma_{\mathrm{n}} / \sigma_{\mathrm{t}}\right)^{1/m} \tag{2}$$

where τ and σ_n respectively are the shear and normal stresses, m is the nonlinear coefficient, c_0 is the initial cohesion and σ_t is the axial tensile stress.

The equivalent cohesion and internal friction angle of nonlinear Mohr-Coulomb failure criterion can be obtained by the tangential technique (Yang and Zou 2011, Yang *et al*. 2013).

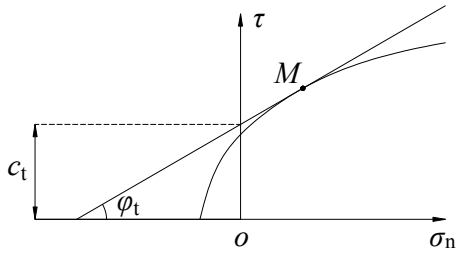

Fig. 1 Tangential line of nonlinear Mohr-Coulomb failure criterion

As illustrated in Fig. 1, the envelope of the nonlinear Mohr-Coulomb failure criterion in stress space is a curve. A tangent line through an arbitrary point on curve M can be expressed as

$$\tau = c_{\mathrm{t}} + \sigma_{\mathrm{n}} \tan \varphi_{\mathrm{t}} \tag{3}$$

where c_t is intercept of the straight line on the τ-axis and φ_t is the corresponding angle with σ_n-axis. c_t and φ_t are the equivalent cohesion and internal friction angle of point M, respectively. The relationship between the equivalent cohesion and internal friction angle is derived by solving Eqs. (2) and (3).

$$c_{\mathrm{t}} = \frac{m-1}{m} c_0 \left(\frac{m\sigma_{\mathrm{t}} \tan \varphi_{\mathrm{t}}}{c_0} \right)^{\frac{1}{1-m}} + \sigma_{\mathrm{t}} \tan \varphi_{\mathrm{t}} \tag{4}$$

According to the research of Chen (1975), upper bound theorem of limit analysis can be represented as: in any kinematically admissible velocity field, the load obtained by equating the external rate of work to the energy dissipation rate is no less than the actual collapse load, which can be expressed as

$$\int_V \sigma_{ij} \dot{\varepsilon}_{ij} \mathrm{d}V \geq \int_S T_i v_i \mathrm{d}S + \int_V F_i v_i \mathrm{d}V \tag{5}$$

in which the left side of the inequality represents the energy dissipation rate of stress σ_{ij} in virtual strain field $\dot{\varepsilon}_{ij}$, the right side denotes the work rates of external loads T_i and body forces F_i in velocity field v_i. The volume of the strain field is V and relevant boundary is S.

The nonlinear Mohr-Coulomb failure criterion is then introduced into the upper bound theorem of limit analysis by substituting Eq. (4) into Eq. (5), and the obtained solution must be an upper bound solution of the actual value.

3. Definition and calculation of model

3.1 New horn failure mechanism

The stability of tunnel face is a three-dimensional problem in practical engineering (Panji *et al*. 2016). Michalowski (Michalowski 2010, Michalowski and Nadukuru 2013) regarded the cross section of the two-dimensional log-spiral failure mechanism as circles with gradual changing diameter. In this work the three-dimensional failure mechanism of tunnel face in soil masses is constructed grounding on this approach. It is called the new horn failure mechanism, as illustrated in Fig. 2. Circle AB is the tunnel face with diameter d. In the excavation process, due to poor soil and disturbance, the soil mass in front of tunnel face tends to collapse. The collapsing block AEB rotates around point O in clockwise direction. AE and BE are log-spiral curves and they together with point O are on the central plane. The length of OA and OB respectively are r_a and r_b, and the angles between OB, OA, OE and vertical direction respectively are θ_1, θ_2 and θ_3. Draw a straight line through point O intersects with AE and BE, the distances between point O and the intersection points are r_1 and r_2, respectively. Taking the distance of the two intersection points as diameter, a series of circles perpendicular to the central plane are drawn. It is the cross section of the horn and the distance between point O and circle center is r_m.

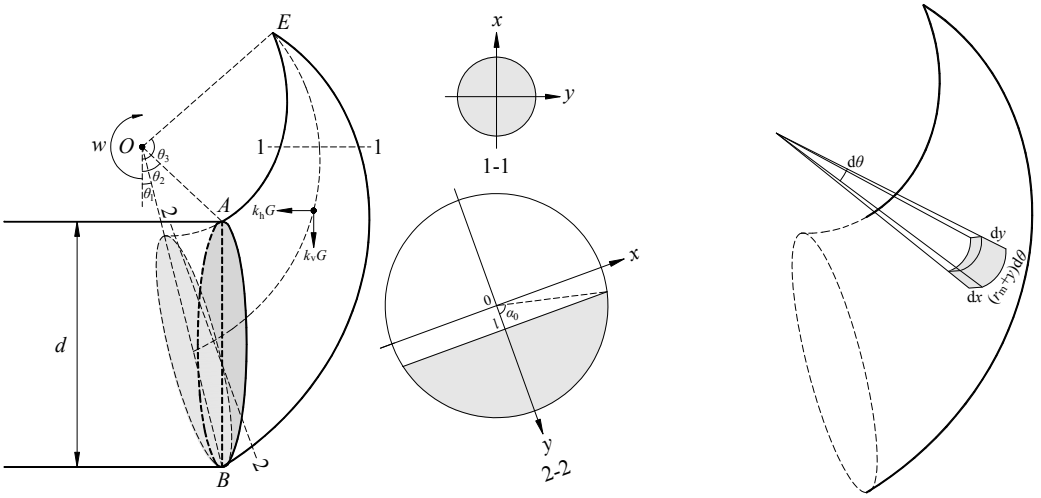

(a) Three-dimensional failure mechanism (b) Microelement volume

Fig. 2 Calculation model of collapse failure of tunnel face

According to the assumption of limit analysis and the nonlinear failure criterion, the angle between the velocity and tangent line on an arbitrary point of the log-spiral curve is φ_t. Thus, the expressions of *AE* and *BE* log-spiral curves respectively are as

$$r_1(\theta) = r_a \exp[(\theta - \theta_2)\tan\varphi_t] \tag{6}$$

$$r_2(\theta) = r_b \exp[(\theta_1 - \theta)\tan\varphi_t] \tag{7}$$

According to the geometric relationship, there are

$$r_a = \frac{\sin\theta_1}{\sin(\theta_2 - \theta_1)} d \tag{8}$$

$$r_b = \frac{\sin\theta_2}{\sin(\theta_2 - \theta_1)} d \tag{9}$$

$$\theta_3 = \frac{1}{2}[(\theta_1 + \theta_2) - \frac{\ln(\sin\theta_1 / \sin\theta_2)}{\tan\varphi_t}] \tag{10}$$

The distance between point *O* and the circle center of cross section is

$$r_m = (r_1 + r_2)/2 \tag{11}$$

The diameter of the cross section is

$$R = (r_2 - r_1)/2 \tag{12}$$

A coordinate system is established in the cross section, which takes the direction from point O to the circle center as the positive direction of y-axis. As illustrated in the cross section 2-2 of Fig. 2(a), α is the angle between the arbitrary point of the circle and the positive direction of y-axis, v denotes the velocity and dV represents the volume of microelement. Assuming the angle of endpoint of arc is α_0 and corresponding y-coordinate is l, following equations can be derived

$$\cos\alpha_0 = l/R \tag{13}$$

$$r_{\mathrm{m}} + l = r_{\mathrm{a}} \cdot \sin\theta_2 / \sin\theta \tag{14}$$

$$v = \omega \cdot \left(r_{\mathrm{m}} + y\right) \tag{15}$$

$$\mathrm{d}V = \left(r_{\mathrm{m}} + y\right) \cdot \mathrm{d}x \cdot \mathrm{d}y \cdot \mathrm{d}\theta \tag{16}$$

3.2 Upper bound solution of the collapse pressure

According to upper bound theorem of limit analysis, following assumptions are made: (1) the soil mass is ideal elastic-plastic material and it obeys the associated flow rule; (2) the horn is rigid and no volumetric stain occurs, therefore energy dissipation is just along the velocity discontinuity lines; (3) the tunnel is deep-buried and apex of the horn is always below the ground; (4) when the failure of tunnel face occurs, the collapse pressure σ_0 is assumed to be uniformly distributed. Moreover, the minimum supporting pressure σ_{T0} is introduced to obtain the collapse pressure. Under the limit state, the minimum supporting pressure is balanced with collapse pressure, namely $\sigma_{T0} = \sigma_0$.

3.2.1 External rate of work and internal energy dissipation

When the failure of tunnel face occurs, the external rate of work includes the work rate of the horn produced by weight $\dot{W}_1$, the rate of work of seismic force $\dot{W}_2$ and the work rate of supporting pressure $\dot{W}_3$. Besides, the internal energy dissipation D is only along the surface of the horn.

The work rate of the self-weight of the horn is

$$\begin{aligned}\dot{W}_1 = &\int_{\theta_2}^{\theta_3} \mathrm{d}\theta \int_{-R}^{R} \mathrm{d}y \int_0^{\sqrt{R^2-y^2}} 2 \cdot \omega \cdot \gamma \cdot \left(r_{\mathrm{m}} + y\right)^2 \cdot \sin\theta \mathrm{d}x + \\ &\int_{\theta_1}^{\theta_2} \mathrm{d}\theta \int_{l}^{R} \mathrm{d}y \int_0^{\sqrt{R^2-y^2}} 2 \cdot \omega \cdot \gamma \cdot \left(r_{\mathrm{m}} + y\right)^2 \cdot \sin\theta \mathrm{d}x\end{aligned} \tag{17}$$

Based on the quasi-static method, the seismic force is equivalent to horizontal seismic force k_hG and vertical seismic force k_vG applying on the horn. The total rate of wok of the horizontal and vertical seismic forces is

$$\begin{aligned}\dot{W}_2 = &k_{\mathrm{v}} \cdot \int_{\theta_2}^{\theta_3} \mathrm{d}\theta \int_{-R}^{R} \mathrm{d}y \int_0^{\sqrt{R^2-y^2}} 2 \cdot \omega \cdot \gamma \cdot \left(r_{\mathrm{m}} + y\right)^2 \cdot \sin\theta \mathrm{d}x + \\ &k_{\mathrm{v}} \cdot \int_{\theta_1}^{\theta_2} \mathrm{d}\theta \int_{l}^{R} \mathrm{d}y \int_0^{\sqrt{R^2-y^2}} 2 \cdot \omega \cdot \gamma \cdot \left(r_{\mathrm{m}} + y\right)^2 \cdot \sin\theta \mathrm{d}x +\end{aligned} \tag{18}$$

$$k_{\mathrm{h}} \cdot \int_{\theta_2}^{\theta_3} \mathrm{d}\theta \int_{-R}^{R} \mathrm{d}y \int_{0}^{\sqrt{R^2-y^2}} 2 \cdot \omega \cdot \gamma \cdot \left(r_{\mathrm{m}} + y\right)^2 \cdot \cos\theta \mathrm{d}x + k_{\mathrm{h}} \cdot \int_{\theta_1}^{\theta_2} \mathrm{d}\theta \int_{l}^{R} \mathrm{d}y \int_{0}^{\sqrt{R^2-y^2}} 2 \cdot \omega \cdot \gamma \cdot \left(r_{\mathrm{m}} + y\right)^2 \cdot \cos\theta \mathrm{d}x \tag{18}$$

The work rate of supporting pressure is

$$\dot{W}_3 = -\sigma_{\mathrm{T0}} \cdot \int_{\theta_1}^{\theta_2} \mathrm{d}\theta \int_{0}^{\sqrt{R^2-l^2}} 2 \cdot \omega \cdot \left(r_{\mathrm{m}} + l\right)^2 \cdot \cos\theta \Big/ \sin\theta \mathrm{d}x \tag{19}$$

The area of intersecting plane between the horn and tunnel face is

$$S_{\mathrm{AB}} = \int_{\theta_1}^{\theta_2} \mathrm{d}\theta \int_{0}^{\sqrt{R^2-l^2}} 2 \cdot \left(r_{\mathrm{m}} + l\right) \Big/ \sin\theta \mathrm{d}x \tag{20}$$

The rate of internal energy dissipation along surface of the horn is

$$D = \int_{\theta_2}^{\theta_3} \mathrm{d}\theta \int_{0}^{\pi} 2 \cdot \omega \cdot c_{\mathrm{t}} \cdot R \cdot \left(r_{\mathrm{m}} + R \cdot \cos\alpha\right)^2 \mathrm{d}\alpha + \int_{\theta_1}^{\theta_2} \mathrm{d}\theta \int_{0}^{\alpha_0} 2 \cdot \omega \cdot c_{\mathrm{t}} \cdot R \cdot \left(r_{\mathrm{m}} + R \cdot \cos\alpha\right)^2 \mathrm{d}\alpha \tag{21}$$

3.2.2 Optimization

The collapse pressure equals to the minimum supporting pressure at limit state. According to the virtual power principle, the minimum supporting pressure can be determined by equating the external rate of work to the rate of internal energy dissipation. Thus, using Eqs. (17), (18), (19) and (21), the expression of the minimum supporting pressure or surrounding pressure is obtained as follows

$$\sigma_0 = \sigma_{\mathrm{T0}} = \frac{\dot{W}_1 + \dot{W}_2 - D}{\int_{\theta_1}^{\theta_2} \mathrm{d}\theta \int_{0}^{\sqrt{R^2-l^2}} 2 \cdot \omega \cdot \left(r_{\mathrm{m}} + l\right)^2 \cdot \cos\theta \Big/ \sin\theta \mathrm{d}x} \tag{22}$$

The constraints of Eq. (22) are

$$\text{s.t.} \begin{cases} 0 < \theta_1 < \theta_2 < \pi / 2 \\ \theta_2 < \theta_3 < \pi \\ r_{\mathrm{a}} < r_{\mathrm{b}} \end{cases} \tag{23}$$

In order to ensure the stability of tunnel face, the maximum collapse pressure at limit state should be solved. As expressed in Eq. (22), the collapse pressure is a function of parameters θ_1, θ_2 and φ_t, namely $\sigma_0 = f(\theta_1, \theta_2, \varphi_t)$. Under this circumstance, the problem can be transformed into a mathematical optimization model. And the optimal upper bound solution of collapse pressure, or referred to as the minimum supporting pressure, can be obtained by virtue of the numerical method. In this paper, the SQP algorithm is employed, which is an effective approach to address the nonlinear constrained programming problems. This algorithm is essentially an iteration algorithm and its main idea is to convert the original issue into a series of quadratic programming problems.

The final solution of the original problem is then obtained when each sub-problem is solved step-by-step.

3.3 Reliability model of tunnel face

The collapse pressure when tunnel face fails is obtained in the previous section. In order to satisfy supporting design, the supporting pressure under different safety levels should be solved.

By introducing a safety factor F_s, the supporting pressure is obtained on the basis of the collapse pressure

$$\sigma_{\mathrm{T}} = F_{\mathrm{s}} \cdot \sigma_0 \tag{24}$$

Considering the randomness of soil parameters and loads, the limit state equation of tunnel face is established as

$$g(X) = \sigma_{\mathrm{T}} - \sigma_0 = 0 \tag{25}$$

In order to ensure the safety of tunnel face, the performance function should satisfy the following equation.

$$g(X) = \sigma_{\mathrm{T}} - \sigma_0 > 0 \tag{26}$$

Thus, the reliability model of tunnel face is

$$R_{\mathrm{s}} = P\{g(X) > 0\} \tag{27}$$

$$P_{\mathrm{f}} = 1 - R_{\mathrm{s}} \tag{28}$$

$$\beta = -\Phi^{-1}(P_{\mathrm{f}}) \tag{29}$$

where R_s is the reliability, P_f is the failure probability and β is the reliability index.

4. Comparison with existing results

Mollon *et al*. (2010) constructed a translational three-dimensional multi-block failure mechanism

Table 1 Comparison between the present work and Mollon *et al*. (2010)

d /m	γ /kN/m^3	c /kPa	φ /°	σ_0 /kPa		
				Mollon *et al*. (2010) (n = 5)	This paper (m = 1)	Difference
10	18.0	7	17	34.48	33.52	-0.96
10	18.0	10	25	10.88	10.74	-0.14
5	16.1	5	38	0.40	0.40	0
5	15.3	5	38	0.10	0.06	-0.04
10	16.0	5	38	7.10	7.11	0.01
13	16.2	5	38	11.40	11.38	-0.02
10	16.0	5	42	5.00	5.25	0.25
13	16.2	5	42	8.30	8.66	0.36

of tunnel face by virtue of a spatial discretization technique. Through calculation, the optimal number of blocks was found to be five, which may not only satisfy the requirement of accuracy, but also consume less computation time. Subsequently, the collapse pressure of tunnel face under linear Mohr-Coulomb failure criterion was obtained in the case of n = 5. By designating m = 1, the nonlinear Mohr-Coulomb failure criterion degrades into the linear one, and under the same geological conditions, corresponding collapse pressure is also calculated by the method presented in this paper. Comparison between the results of this paper and Mollon *et al*. (2010) are illustrated in Table 1. It is found they are essentially the same and the maximum difference is only -0.96 kPa. Consequently, the presented method is demonstrated to be valid.

5. Limit analysis of static stability

The stability of tunnel face under the static condition is investigated by virtue of nonlinear limit analysis, namely taking no account of the seismic effect. The influences of nonlinear coefficient and initial cohesion on collapse pressure are illustrated in Fig. 3. It can be found that, when initial cohesion c_0 is constant, the collapse pressure σ_0 increases almost linearly with the increase of nonlinear coefficient m. The increment is greater when initial cohesion is smaller. However, when the nonlinear coefficient m is a constant, the collapse pressure σ_0 increases with the decrease of initial cohesion c_0. The increment is greater when nonlinear coefficient is larger.

Figs. 4 and 5 illustrate the influences of nonlinear coefficient and initial cohesion on failure mechanism, respectively. It can be found that, with the increase of nonlinear coefficient or the decrease of initial cohesion, the failure zone and height of failure mechanism increase, which means the horn is bigger and the failure mechanism tends to move upward and forward. Thus, the intensity and range of the advance support should be increased in the support design, and corresponding elevation angle ought to be properly increased. It can be concluded that a bigger nonlinear coefficient or a smaller initial cohesion indicates poor soil quality, and the collapse pressure together with failure zone is larger during the excavation. Under this circumstance, supporting pressure and supporting range should be bigger to ensure the stability of tunnel face.

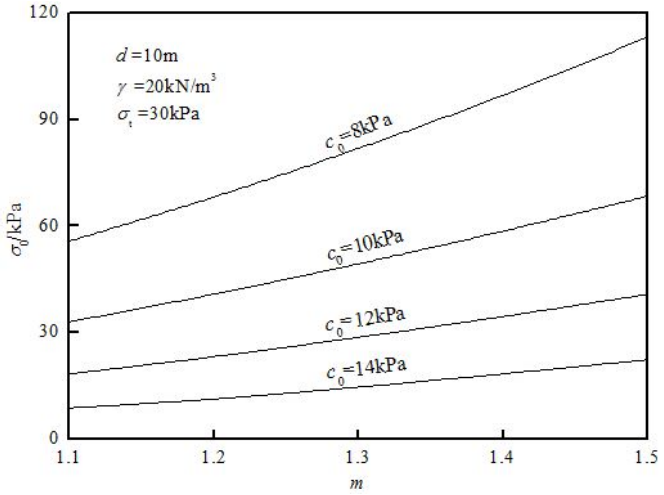

Fig. 3 Influences of nonlinear coefficient and initial cohesion on the collapse pressure

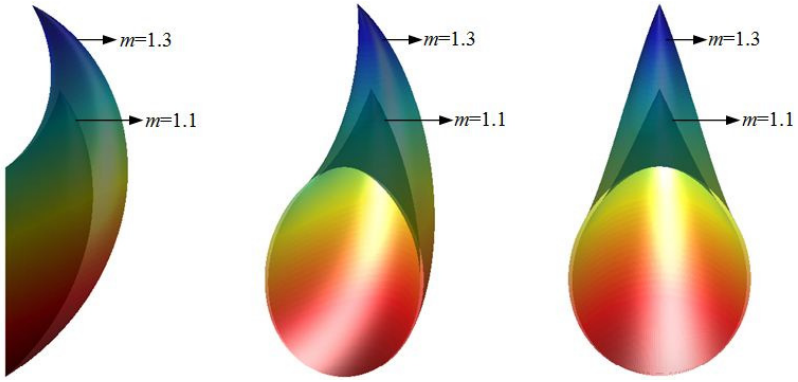

Fig. 4 Influence of nonlinear coefficient on the failure mechanism
(d = 10 m, γ = 20 kN/m^3, c_0 = 14 kPa, σ_t = 30 kPa, k_h = 0, ζ = 0)

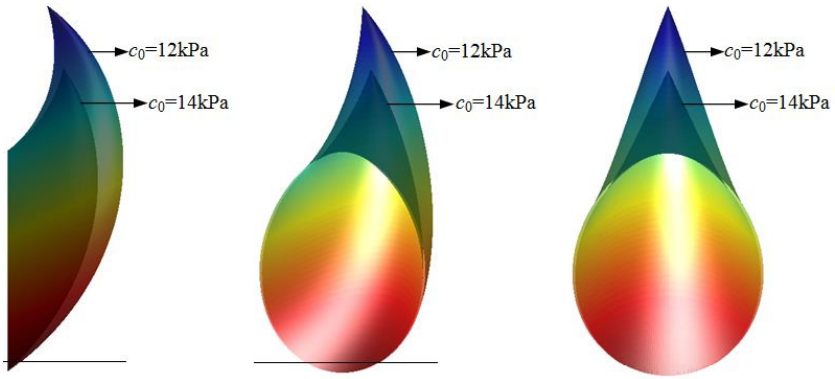

Fig. 5 Influence of initial cohesion on the failure mechanism
(d = 10 m, γ = 20 kN/m^3, m = 1.1, σ_t = 30 kPa, k_h = 0, ζ = 0)

6. Limit analysis of dynamic stability using quasi-static method

The seismic force is introduced into the limit analysis by virtue of quasi-static method. In order to investigate the influences of horizontal and vertical seismic forces on the stability of tunnel face separately, the two conditions are discussed, which includes (1) horizontal seismic action; (2) horizontal and vertical seismic action.

6.1 Horizontal seismic action

The stability of tunnel face subjected to horizontal seismic force is investigated using the nonlinear limit analysis. The influence of horizontal seismic coefficient on collapse pressure is illustrated in Fig. 6. It is found that the collapse pressure σ_0 increases linearly with the increase of horizontal seismic coefficient k_h and soil unit weight γ. A bigger value of horizontal seismic coefficient or soil unit weight results in a bigger horizontal seismic force obtained by quasi-static method. Thus, the horizontal seismic force has a significant influence on the collapse pressure of tunnel face. Fig. 7 illustrates the influence of horizontal seismic coefficient on failure mechanism.

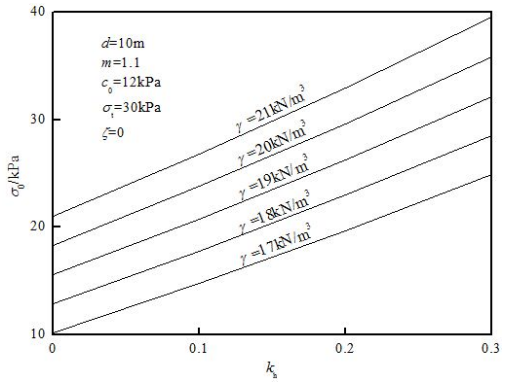

Fig. 6 Influences of horizontal seismic coefficient and soil unit weight on the collapse pressure

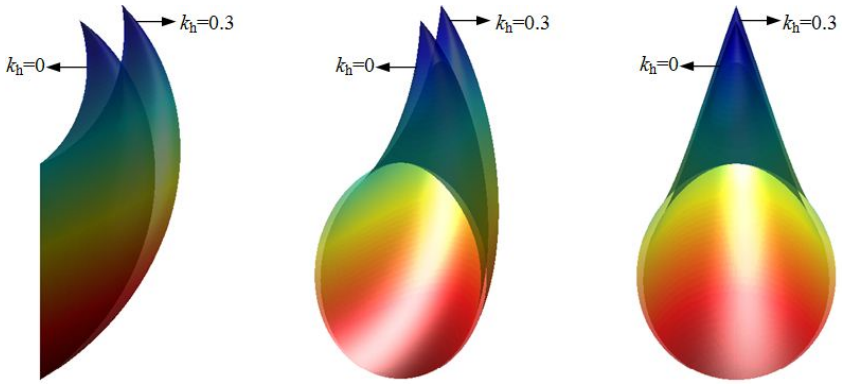

Fig. 7 Influence of horizontal seismic coefficient on the failure mechanism
(d = 10 m, γ = 20 kN/m^3, m = 1.1, c_0 = 12 kPa, σ_t = 30 kPa, ζ = 0)

It can be found that, with the increase of horizontal seismic coefficient k_h, the failure mechanism tends to move upward and forward, and the failure zone and height of failure mechanism slightly increase. Under this circumstance, it is suggested to increase the length of rock bolt and decrease corresponding elevation angle.

6.2 Horizontal and vertical seismic action

The existing researches related to the stability of geotechnical structure focuses on the horizontal dynamic effect of seismic force, while the vertical dynamic effect is usually ignored. However, when the earthquake intensity is high, the influence of vertical dynamic effect of seismic force on the stability of geotechnical structure should not be neglected (Alielahi and Adampira 2016c). Thus, this section takes both the horizontal and vertical seismic force into account, and investigates the stability of tunnel face by nonlinear limit analysis. The influence of vertical seismic proportional coefficient on collapse pressure is illustrated in Fig. 8. It can be found that, when the horizontal seismic coefficient is constant ($k_h \neq 0$), the collapse pressure σ_0 will increase linearly with the enlargement of vertical seismic proportional coefficient. The increment is greater when the horizontal seismic coefficient is bigger. Fig. 9 illustrates the influence of vertical seismic

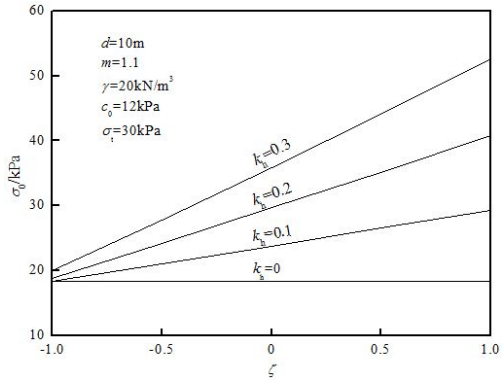

Fig. 8 Influence of vertical seismic proportional coefficient on the collapse pressure

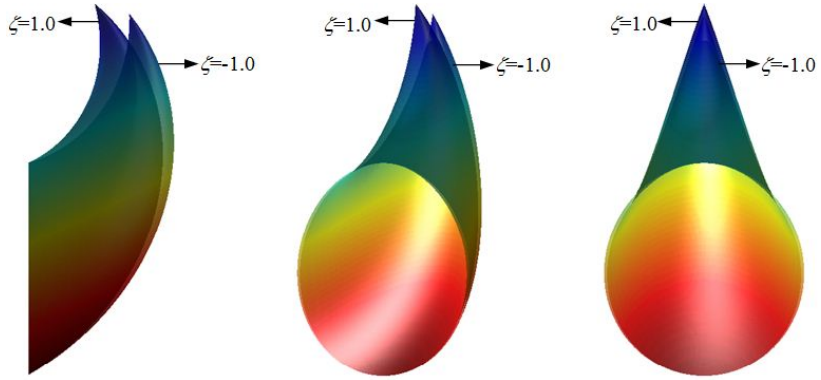

Fig. 9 Influence of vertical seismic proportional coefficient on the failure mechanism (d = 10 m, γ = 20 kN/m^3, m = 1.1, c_0 = 12 kPa, σ_t = 30 kPa, k_h = 0.3)

proportional coefficient on failure mechanism. It can be found that, with the increase of vertical seismic proportional coefficient, the failure mechanism tends to move backward and upward, and the failure zone and height of failure mechanism slightly increase. Under this circumstance, it is suggested to decrease the length of rock bolt and increase corresponding elevation angle. It can be concluded that the vertical seismic force has significant effect on the collapse pressure and failure mechanism. This effect is closely linked to horizontal seismic force and should not be ignored.

7. Reliability analysis

Taking the randomness of soil parameters and loads into consideration, this section investigates the influences of horizontal and vertical seismic force on the stability of tunnel face using reliability theory. The diameter of tunnel face is d = 10 m and the statistical characteristic of soil parameters and loads is shown in Table 2. The target reliability indexes [β] at different safety levels are shown in Table 3.

Considering the simultaneous action of horizontal and vertical seismic forces, for different horizontal seismic coefficients and vertical seismic proportional coefficients, the relationship

Table 2 Statistical property of random variables

Random variable	Mean	Standard deviation	Coefficient of variation	Distribution type
m	1.4	0.21	0.15	Gaussian
c_0 /kPa	10	1.5	0.15	Gaussian
σ_t /kPa	30	4.5	0.15	Gaussian
γ /kN/m^3	20	3	0.15	Gaussian
k_h	0~0.3	—	0.15	Gaussian
ζ	-1.0~1.0	—	0.15	Gaussian
σ_T /kPa	—	—	0.15	Gaussian

Table 3 Target reliability index of tunnel structure

Type of limit state		Safety classes		
		1	2	3
Serviceability limit state		1.0~2.5		
Ultimate limit state	Brittle failure	4.7	4.2	3.7
	Ductile failure	4.2	3.7	3.2

between failure probability and safety factor are illustrated in Figs. 10 and 11. It is obvious that, with the increase of safety factor F_s, the failure probability P_f decreases. When safety factor is bigger, the decrease is slower. Thus, reasonably increasing the safety factor will effectively reduce the failure risk of tunnel face. However, in order not to waste the resources, the safety factor should not be too large. Moreover, the fluctuation amplitude of failure probability curve increases with the increase of safety factor F_s. The increase is more obvious when the failure probability is less than 10^{-5}. This is because the obtained failure probability P_f is big when the value of F_s is small. As a result, the influence of the randomly-generated sample on the failure probability is small and the curve of P_f is nearly a straight line. On the contrary, the magnitude of P_f is small when the value of F_s is big. Under this circumstance, relevant influence of the sample on P_f is big, and thus, the curve of P_f fluctuates. It can be concluded that the size of sample has a certain impact on the computed results. This impact can be ignored when the required computational accuracy is low. However, the impact may be great when a high calculation precision is required. In this case, the size of sample should be increased in order to obtain a better solution. The sample size of this paper is 4 million and the obtained results satisfy the accuracy requirement.

In order to illustrate the influence of horizontal seismic force, the conditions of different magnitudes of horizontal seismic force (k_h = 0~0.3) are compared with the static case. As shown in Table 4, the horizontal seismic coefficient, which determines the magnitude of the horizontal seismic force, has great influences on the collapse pressure σ_0 and supporting pressure σ_T. Comparing with the static condition, the maximum relative error of collapse pressure is 52%. Corresponding to 3 safety levels ([β] = 3.2, [β] = 3.7 and [β] = 4.2), the maximum relative errors of supporting pressure respectively are 40%, 39% and 34%. Similarly, the conditions of different vertical seismic force (ζ = -1.0, -0.5, 0.5, 1.0) are compared with the case with no vertical seismic force (ζ = 0) to illustrate the influence of the vertical seismic force. As shown in Table 5, the vertical seismic proportional coefficient, which determines the magnitude of the vertical seismic

force, has great influences on the collapse pressure σ_0 and supporting pressure σ_T. Comparing with the condition of no vertical seismic force ($\zeta = 0$), the maximum relative error of collapse pressure is 48%. Corresponding to 3 safety levels ($[\beta] = 3.2$, $[\beta] = 3.7$ and $[\beta] = 4.2$), the maximum relative

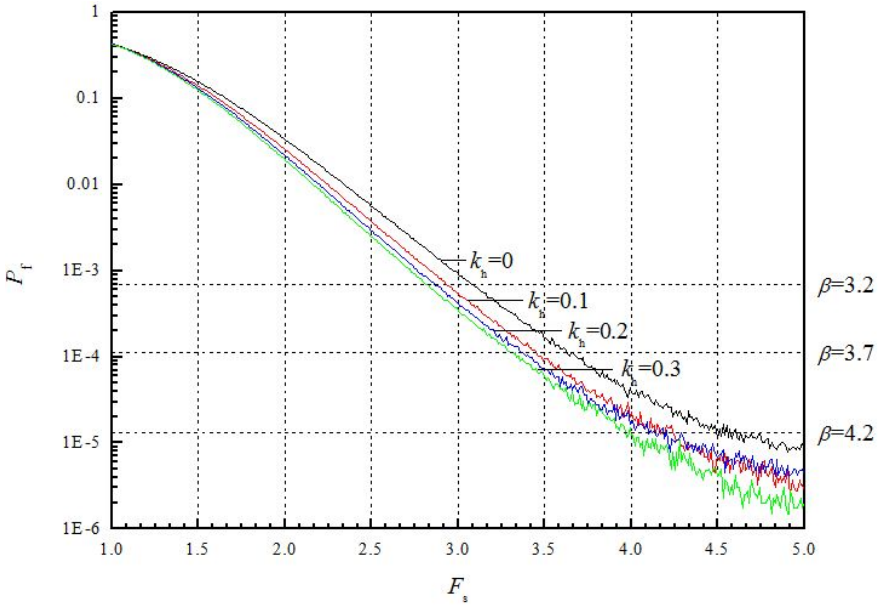

Fig. 10 Influence of safety factor on the failure probability with different horizontal seismic coefficients ($\zeta = 0.5$)

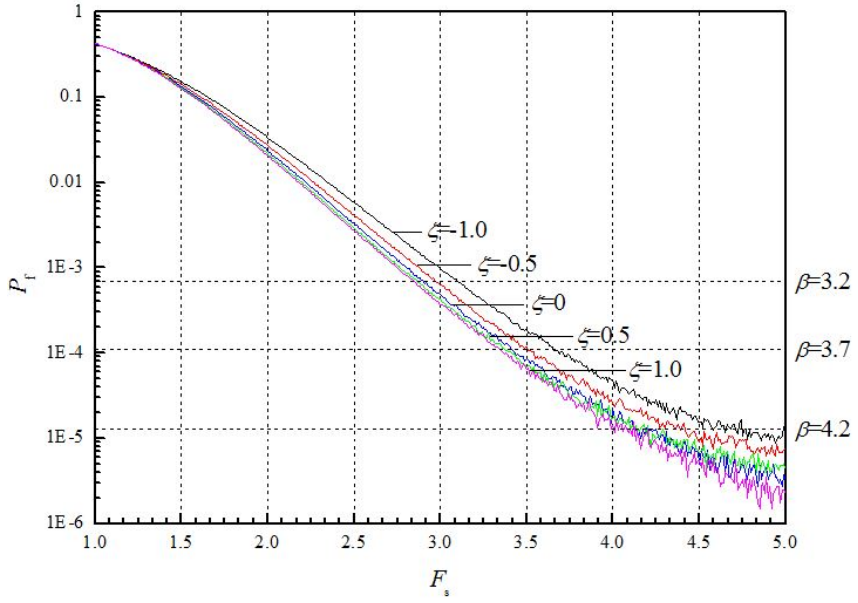

Fig. 11 Influence of safety factor on the failure probability with different vertical seismic proportional coefficients ($k_h = 0.2$)

Table 4 Collapse pressure of tunnel face along with required safety factor and supporting pressure at 3 different safety levels ($\zeta = 0$)

k_h	σ_0 /kPa	Error	[β]								
			3.2			3.7			4.2		
			$F_{s\min}$	$\sigma_{T\min}$ /kPa	Error	$F_{s\min}$	$\sigma_{T\min}$ /kPa	Error	$F_{s\min}$	$\sigma_{T\min}$ /kPa	Error
0	58.5	—	3.08	180.2	—	3.66	214.1	—	4.74	277.3	—
0.1	67.5	15%	2.97	200.5	11%	3.49	235.6	10%	4.39	296.3	7%
0.2	77.5	32%	2.92	226.3	26%	3.43	265.8	24%	4.25	329.4	19%
0.3	88.7	52%	2.84	251.9	40%	3.36	298.0	39%	4.18	370.8	34%

Table 5 Collapse pressure of tunnel face along with required safety factor and supporting pressure at 3 different safety levels

k_h	ζ	σ_0 /kPa	Error	[β]								
				3.2			3.7			4.2		
				$F_{s\min}$	$\sigma_{T\min}$ /kPa	Error	$F_{s\min}$	$\sigma_{T\min}$ /kPa	Error	$F_{s\min}$	$\sigma_{T\min}$ /kPa	Error
0	0	58.5	—	3.08	180.2	—	3.66	214.1	—	4.74	277.3	—
0	-1.0	58.5	0%	3.08	180.2	0%	3.66	214.1	0%	4.74	277.3	0%
0	-0.5	58.5	0%	3.08	180.2	0%	3.66	214.1	0%	4.74	277.3	0%
0	0.5	58.5	0%	3.08	180.2	0%	3.66	214.1	0%	4.74	277.3	0%
0	1.0	58.5	0%	3.08	180.2	0%	3.66	214.1	0%	4.74	277.3	0%
0.1	0	67.5	—	2.97	200.5	—	3.49	235.6	—	4.39	296.3	—
0.1	-1.0	54.5	-19%	3.08	167.9	-16%	3.66	199.5	-15%	4.65	253.4	-14%
0.1	-0.5	60.9	-10%	3.01	183.3	-9%	3.58	218.0	-7%	4.49	273.4	-8%
0.1	0.5	74.2	10%	2.93	217.4	8%	3.45	256.0	9%	4.24	314.6	6%
0.1	1.0	81.0	20%	2.91	235.7	18%	3.43	277.8	18%	4.19	339.4	15%
0.2	0	77.5	—	2.92	226.3	—	3.43	265.8	—	4.25	329.4	—
0.2	-1.0	51.9	-33%	3.10	160.9	-29%	3.67	190.5	-28%	4.77	247.6	-25%
0.2	-0.5	64.4	-17%	2.97	191.3	-15%	3.52	226.7	-15%	4.42	284.6	-14%
0.2	0.5	91.2	18%	2.86	260.8	15%	3.38	308.3	16%	4.16	379.4	15%
0.2	1.0	105.5	36%	2.85	300.7	33%	3.36	354.5	33%	3.99	420.9	28%
0.3	0	88.7	—	2.84	251.9	—	3.36	298.0	—	4.18	370.8	—
0.3	-1.0	51.1	-42%	3.12	159.4	-37%	3.67	187.5	-37%	5.14	262.7	-29%
0.3	-0.5	69.2	-22%	2.93	202.8	-19%	3.46	239.4	-20%	4.45	307.9	-17%
0.3	0.5	109.6	24%	2.82	309.1	23%	3.33	365.0	22%	4.01	439.5	19%
0.3	1.0	131.6	48%	2.81	369.8	47%	3.30	434.3	46%	4.04	531.7	43%

errors of supporting pressure respectively are 47%, 46% and 43%. Therefore, the horizontal and vertical seismic forces have a great impact on the stability of tunnel face. Both the horizontal and vertical seismic forces ought to be taken into account during the supporting design. Furthermore, when conducting seismic design of tunnel, the horizontal seismic coefficient k_h and vertical seismic proportional coefficient ζ should be rationally determined on the basis of different safety

levels. For different horizontal seismic coefficients and vertical seismic proportional coefficients, the collapse pressures together with the required minimum safety factors and supporting pressures under 3 different safety levels are listed in Table 5, which can provide references to the seismic design of tunnels.

8. Conclusions

- Based on the three-dimensional horn failure mechanism and the nonlinear limit analysis theory, upper bound solution for the collapse pressure of tunnel face under seismic action is obtained.
- With the increase of nonlinear coefficient or the decrease of initial cohesion, the collapse pressure, the failure zone and the height of the mechanism increase under static condition. In this case, the intensity along with the range of advance support ought to be increased, and corresponding elevation angle should also be appropriately increased.
- With the increase of horizontal seismic coefficient, the collapse pressure linearly increases and the failure mechanism tends to move forward and upward. The failure zone and the height of mechanism also slightly increase. Under this circumstance, the supporting pressure and the length of anchor stock ought to be increased, while corresponding elevation angle should be decreased. The vertical seismic force also has apparent influences on the collapse pressure and the failure mechanism.
- The reasonable increase of safety factor could efficiently reduce the failure risk of tunnel face. But for the sake of saving resources, the safety factor should not be too large. The influences of horizontal and vertical seismic forces must be simultaneously considered during seismic design. When the horizontal seismic force is not taken into account, the maximum relative error of collapse pressure is 52%. And the maximum relative errors of supporting pressure under 3 safety levels respectively are 40%, 39% and 34%. Analogously, when the vertical seismic force is not taken into consideration, the maximum relative error of collapse pressure is 48%. Relevant maximum relative errors of supporting pressure under 3 safety levels respectively are 47%, 46% and 43%.
- The research results of this paper may provide references to the seismic design of tunnels, and the proposed method also gives a new idea to it. As regards practical engineering, the seismic coefficient along with the target reliability can be determined by making reference to the design codes. And the physical mechanics parameters of soil mass can be obtained through site investigation and laboratory test. Then, based on the method proposed in this paper, the complete supporting design parameters are derived.
- The collapse pressure and the failure zone of tunnel face obtained on the basis of the nonlinear limit analysis theory are more applicable to engineering practice. Meanwhile, the required safety factor and relevant supporting pressure with respect to 3 different safety levels can also provide complete supporting design parameters to the seismic design of tunnels. However, there remains following limitations: (1) the research results are only suitable to tunnels excavated in soil masses due to the nonlinear Mohr-Coulomb failure criterion is adopted; (2) the quasi-static method is a simplified method and the obtained results are not precise enough on account of the dynamic property of earthquake is ignored.

Acknowledgments

The preparation of the paper has received financial supports from National Natural Science Foundation of China (51378514, 51674115 and 51308072) and Scientific Research Foundation for Doctor of Hunan University of Science and Technology (E51768). The financial supports are greatly appreciated.

References

Alielahi, H. and Adampira, M. (2016a), "Effect of twin–parallel tunnels on seismic ground response due to vertically in-plane waves", *Int. J. Rock Mech. Min. Sci.*, **85**, 67-83.

Alielahi, H. and Adampira, M. (2016b), "Seismic effects of two-dimensional subsurface cavity on the ground motion by BEM: Amplification patterns and engineering applications", *Int. J. Civil Eng.*, **14**(4), 233-251.

Alielahi, H. and Adampira, M. (2016c), "Site-specific response spectra for seismic motions in half-plane with shallow cavities", *Soil Dyn. Earthq. Eng.*, **80**, 163-167.

Chen, W.F. (1975), *Limit Analysis and Soil Plasticity*, Elsevier Science, Amsterdam, The Netherlands.

Leca, E. and Dormieux, L. (1990), "Upper and lower bound solutions for the face stability of shallow circular tunnels in frictional material", *Géotechnique*, **40**(4), 581-606.

Liu, X.R., Li, D.L., Wang, J.B. and Wang, Z. (2015), "Surrounding rock pressure of shallow-buried bilateral bias tunnels under earthquake", *Geomech. Eng.*, **9**(4), 427-445.

Michalowski, R.L. (2010), "Limit analysis and stability charts for 3D slope failures", *J. Geotech. Geoenviron. Eng.*, **136**(4), 583-593.

Michalowski, R.L. and Nadukuru, S.S. (2013), "Three–dimensional limit analysis of slopes with pore pressure", *J. Geotech. Geoenviron. Eng.*, **139**(9), 1604-1610.

Mollon, G., Dias, D. and Soubra, A.H. (2010), "Face stability analysis of circular tunnels driven by a pressurized shield", *J. Geotech. Geoenviron. Eng.*, **136**(1), 215-229.

Mollon, G., Dias, D. and Soubra, A.H. (2011), "Rotational failure mechanisms for the face stability analysis of tunnels driven by a pressurized shield", *Int. J. Numer. Anal. Methods Geomech.*, **35**(12), 1363-1388.

Mollon, G., Dias, D. and Soubra, A.H. (2013), "Range of the safe retaining pressures of a pressurized tunnel face by a probabilistic approach", *J. Geotech. Geoenviron. Eng.*, **139**(11), 1954-1967.

Panji, M., Koohsari, H., Adampira, M., Alielahi, H. and Marnani, J.A. (2016), "Stability analysis of shallow tunnels subjected to eccentric loads by a boundary element method", *J. Rock Mech. Geotech. Eng.*, **8**(4), 480-488.

Pitilakis, K., Tsinidis, G., Leanza, A. and Maugeri, M. (2014), "Seismic behaviour of circular tunnels accounting for above ground structures interaction effects", *Soil Dyn. Earthq. Eng.*, **67**(67), 1-15.

Saada, Z., Maghous, S. and Garnier, D. (2013), "Pseudo–static analysis of tunnel face stability using the generalized Hoek–Brown strength criterion", *Int. J. Numer. Anal. Methods Geomech.*, **37**(18), 3194-3212.

Sahoo, J.P. and Kumar, J. (2014), "Stability of a circular tunnel in presence of pseudostatic seismic body forces", *Tunnel. Undergr. Space Technol.*, **42**(5), 264-276.

Shen, Y.S., Gao, B., Yang, X.M. and Tao, S.J. (2014), "Seismic damage mechanism and dynamic deformation characteristic analysis of mountain tunnel after Wenchuan earthquake", *Eng. Geol.*, **180**, 85-98.

Soubra, A.H. (2000), "Three–dimensional face stability analysis of shallow circular tunnels", *Proceedings of International Conference on Geotechnical and Geological Engineering*, International Society for Rock Mechanic, Melbourne, Australia, November.

Soubra, A.H. (2002), "Kinematical approach to the face stability analysis of shallow circular tunnels", *Proceedings of the 8th International Symposium on Plasticity*, British Columbia, Canada, July, pp. 443-445.

Soubra, A.H., Dias, D., Emeriault, F. and Kastner, R. (2008), "Three–dimensional face stability analysis of

circular tunnels by a kinematical approach", *Proceedings of the GeoCongress*, *Characterization*, *Monitoring*, *and Modelling of Geosystems*, New Orleans, LA, USA, March, pp. 9-12.
Subrin, D. and Wong, H. (2002), "Tunnel face stability in frictional material: A new 3D failure mechanism", *Comptes Rendus Mecanique*, **330**(7), 513-519.
Yang, X.L. and Yan, R.M. (2015), "Collapse mechanism for deep tunnel subjected to seepage force in layered soils", *Geomech*. *Eng*., *Int*. *J*., **8**(5), 741-756.
Yang, X.L. and Zou, J.F. (2011), "Cavity expansion analysis with non–linear failure criterion", *P*. *I*. *Civil Eng*.-*Geotec*., **164**(1), 41-49.
Yang, X.L., Yang, Z.H., Li, Y.X. and Li, S.C. (2013), "Upper bound solution for supporting pressure acting on shallow tunnel based on modified tangential technique", *J*. *Central South Univ*., **20**(12), 3676-3682.
Zhang, J.H., Xu, J.S. and Zhang, B. (2014), "Energy analysis of stability of twin shallow tunnels based on nonlinear failure criterion", *J*. *Central South Univ*., **21**(12), 4669-4676.

CC